Simulation of cooling induced residual stress distribution in diamond layers on steel

M. Penzel[1], R. Börner[1], F. Müller[1], M. Zinecker[1], A. Schubert[1]
[1]Professorship Micromanufacturing Technology, Chemnitz University of Technology, 09107 Chemnitz, Germany

Abstract

Diamond is a modification of carbon and so far one of the hardest known materials. It is well suitable as a protection layer on various materials for high erosive, mechanical or chemical load. For example, CVD diamond coated tools provide high wear resistance, extended tool life, and good surface quality. [1] In this research steel is used as substrate material since it is easy to machine in comparison to other materials, low in price and it has a high strength and toughness. The hot filament chemical vapour deposition process (HF-CVD) was established as the most important diamond coating process for the homogeneous coating of mechanical parts like bearings or tools, for example 3D freeform surfaces or aluminium die-casting tools. In the HF-CVD process, a methane-containing hydrogen atmosphere is excited at hot tungsten carbide wires which are heated. During the coating process both materials steel and diamond reach typical temperatures between 750 °C and 950 °C.
There is a major challenge in CVD diamond coating on steel materials that has to be faced. Both materials show very different coefficients of thermal expansion. By cooling from the coating temperature to room temperature different strains and high residual compressive stresses appear in the diamond layer, often causing a spontaneous buckling or spalling of the diamond layer. [2–4] The investigations in this paper aim for a defined surface design that can reduce the generation of residual stresses in the coating.
This paper will describe the setup of simulations for cooling and residual stress analysis in coated and surface structured materials. Through the use of the simulation software COMSOL Multiphysics, 2D models were developed to simulate the cooling process of a coated substrate material (AISI 4340) from 900 °C down to 20 °C. For the setup of the models, the modules "Solid Mechanics", "Heat Transport in Solids", the condition "Thermal Expansion" and "Coupling of Temperatures" were used. In the simulations a monolayer of CVD diamond with a minimum thickness of 2 µm is applied on top of the substrate material. Meshing is done with triangular elements to allow easy mesh displacement in any direction. The residual stress was evaluated in the steel domain, the diamond domain and in the interface. The interface between the substrate and the diamond layer is of particular interest in these simulations to gain more detailed knowledge about excessive compressive stresses within the diamond layer to prevent delamination. For this reason the structure of the interface was varied and investigated.

Introduction

Coatings are used in industrial and technical applications to reduce friction and to protect against wear. One of the most common known coatings is diamond like carbon (DLC). [1]
The coating of steel surfaces with CVD diamond has so far not been adequate successful, due to the induced residual stress during the cooling process. To realise diamond coatings on steel, a deeper understanding of the adhesion mechanisms, which are highly influenced by the interlayer, the morphology of the diamond layer, the CVD diamond coating parameters as well as the substrate surface finish, is required. The simulation of the cooling process will help to understand the cooling induced stress distribution in the diamond layer on steel. The investigations are aimed at a defined surface design, which can manipulate the generation of residual stresses in the substrate, the interface and the coating. Therefore, 2D simulation models are created using the “heat transfer in solids” and the “Solid Mechanics” modules.

Geometry

Figure 1 shows an example of a surface manufactured with vibration superimposed milling in the ultrasonic range. [5]

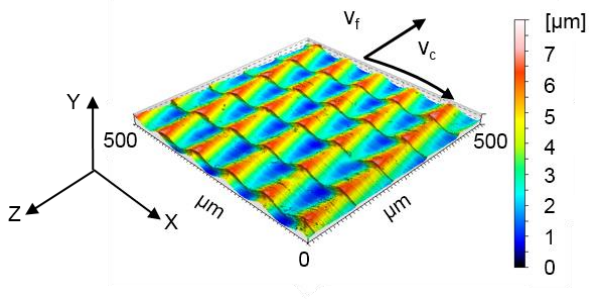

Figure 1: Example of surface created by ultrasonic vibration superimposed milling [5]

The cross cut section of the surface shown in Figure 1 was transferred as parametric geometry into

COMSOL Multiphysics. The setup of the implemented 2D geometry is shown in Figure 2.

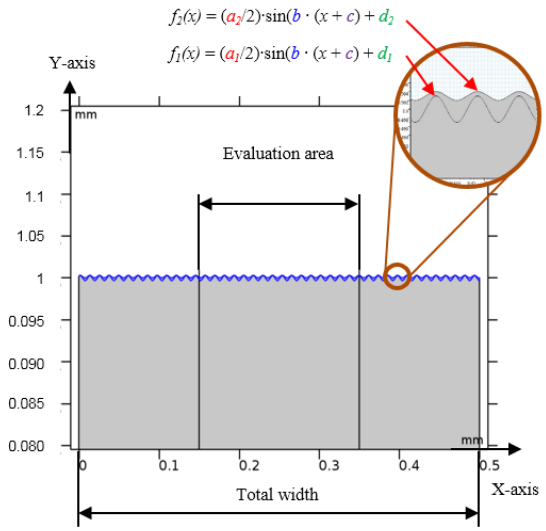

Figure 2: Schematic representation of the transferred 2D geometry

The top of the 2D geometry is defined by two functions. In this context $f_1(x)$ denotes the surface structure of the interface between the steel (AISI 4034) and the diamond. Furthermore $f_2(x)$ characterizes the surface of the diamond coating. The structure of the sinus functions is given in equation (1) and equation (2).

$$f_1(x) = \left(\frac{a_1}{2}\right) \cdot \sin\left(b \cdot (x + c)\right) + d_1 \qquad (1)$$

$$f_2(x) = \left(\frac{a_2}{2}\right) \cdot \sin\left(b \cdot (x + c)\right) + d_2 \qquad (2)$$

The sinus functions can be changed in various ways. They can be shifted, stretched, or compressed in the x- and y-direction. The parameters a_x, b, c, d determine how the graph is exactly changed. The parameter a_x is used for stretching or compressing in y-direction, b is changing the period of the function, c changes the position of the graph in x-direction and the parameter d shifts the sinus along the y-axis. [6]
The total height of the geometry is 1 mm, the total width is 0.5 mm and the thickness D of the diamond layer is 2 µm measured from high peak to high peak of the two functions $f_1(x)$ and $f_2(x)$. Table 1 shows an example of expressions used in the simulations.

Table 1: Parameter examples for the model geometry

Name	Expression	Description
a_1	4 [µm]	stretching or compressing in y-direction
a_2	1 [µm]	stretching or compressing in y-direction
p	12, 24, 48, 96 [µm]	stretching or compressing in x-direction
b	$2\pi/p$	stretching or compressing in x-direction
c	0	shift in x-direction
d_1	1 [mm]	shift in y-direction
d_2	$1+a_1+D-a_2$ [mm]	shift in y-direction

Material and Mesh

The areas for the material definition of diamond and steel and also the mesh are shown as enlarged detail in Figure 3.

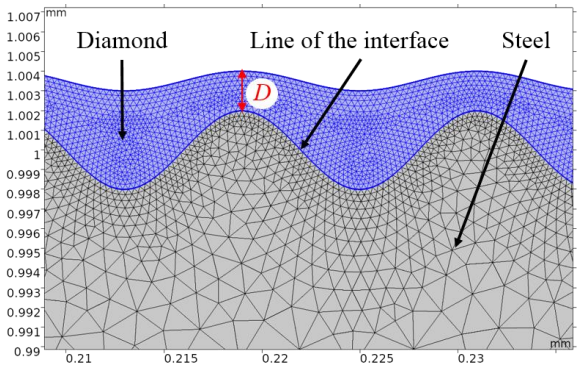

Figure 3: Detailed view to domains and mesh distribution

Furthermore, Figure 3 shows the diamond layer on top of the steel substrate. The material properties for diamond and the specific steel can be found in the material library from COMSOL Multiphysics. For a smooth mesh distribution in the diamond layer the interface line between the diamond and the steel body is defined to a maximum element size of 0.3 µm. The total number of mesh elements was 83047 with an average element quality of 89 %, in this case.

Physics

For the setup of the models, the modules "Solid Mechanics", "Heat Transport in Solids", the condition "Thermal Expansion" and "Coupling of Temperatures" are used.
In “Solid Mechanics” both domains will be considered as linear elastic material. The top line of the steel is

defined with free movement to realize that no restrictions and loads act on the boundary layer.
"Heat Transfer in Solids" is applied to both domains diamond and steel. For both domains the room temperature was defined 20 °C. Heat flux is applied to all outer edges so thermal energy can dissipate to the surroundings.
In the multiphysics intersection "Thermal Expansion" the temperature of 900 °C is defined as volume temperature. The period length, parameter p, is added as "Parametric Sweep" to the "Study".

Results

In COMSOL Multiphysics the values of principle stresses are ordered in such that $\sigma_1 > \sigma_2 > \sigma_3$. This allows to evaluate the following expression in the surface plots:

$$if(abs(solid.sp_1) > abs(solid.sp_3), solid.sp_1, solid.sp_3).$$

For the evaluation of the simulation results it is necessary to know that compressive stresses are defined by negative and tensile stress by positive values. The interface between the steel body and the diamond layer is of special interest. Therefore, the magnitudes of principle stress, shear stress and normal stress were evaluated here. Different from reality the substrate microstructure in the interface has a superimposed sub-roughness which is neglected in the simulations as a simplification.
Figure 4 shows the principal stresses in the area of evaluation as an enlarged illustration for p = 12 µm.

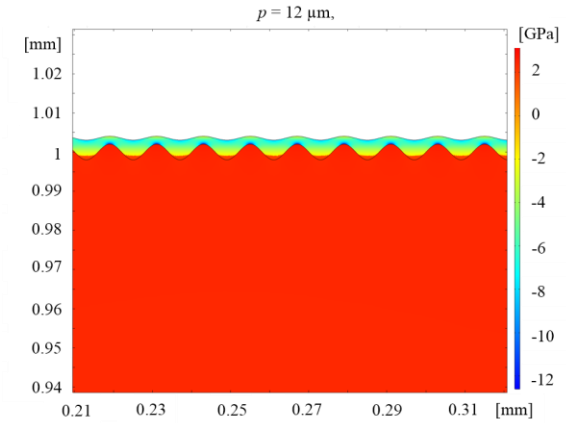

Figure 4: Illustration of the principle stress distribution for p = 12 µm

In Figure 4 the absolute maximum principle stress can be derived in the diamond layer above the upper vertexes of the steel surface. In this diamond layer this stress shows a value of $\sigma_3 = -12.57$ GPa. At the lower vertex of $f_1(x)$, in the diamond layer tensile stress with a value of 1.92 GPa can be found. The maximum shear stress at the line between the steel and the diamond is $\tau = 1.51$ GPa and the normal stress is calculated with a value of $\sigma_n = 2.07$ GPa.
In comparison the results for p = 24 are shown in Figure 5.

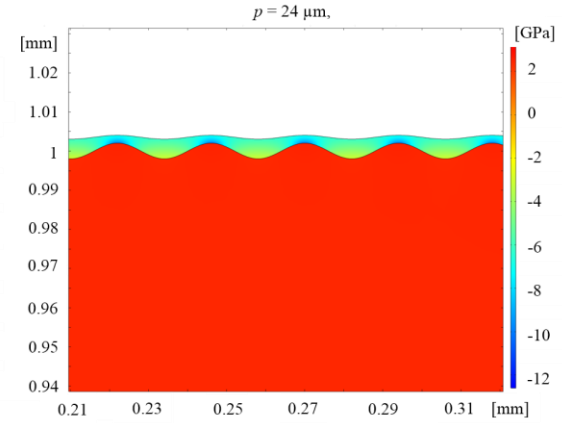

Figure 5: Illustration of the principle stress distribution for p = 24 µm

The maximum principle stress is located in the diamond layer above the upper vertexes of the steel surface with a value of $\sigma_3 = -9.99$ GPa. The maximum shear stress at the line between the steel and the diamond is $\tau = 0.79$ GPa and the normal stress is calculated with a value of $\sigma_n = 1.08$ GPa. In comparison to p = 12, no tensile stress occurs in the diamond layer.
The resulting absolute values for p = 48 µm are shown in Figure 6.

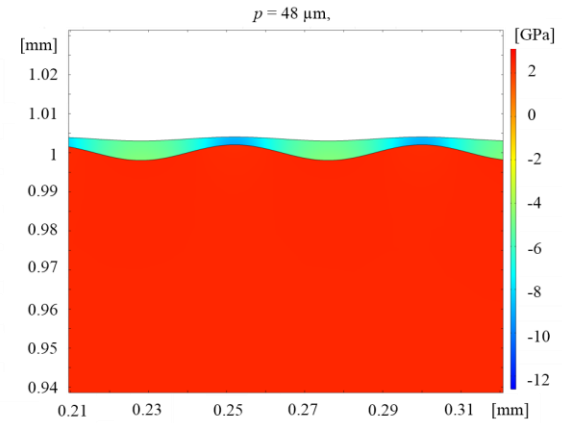

Figure 6: Illustration of the principle stress distribution for p = 48 µm

The maximum principle stress can be found in the diamond layer above the upper vertexes of the steel surface. For the period of p = 48 µm the maximum principle stress is $\sigma_3 = -9.08$ GPa. The maximum shear stress between the diamond layer and the steel surface is $\tau = 0.42$ GPa and normal stress between both materials is $\sigma_n = 0.31$ GPa.
The last evaluated value is p = 96 µm. The result of the resulting principle stress is shown in Figure 7.

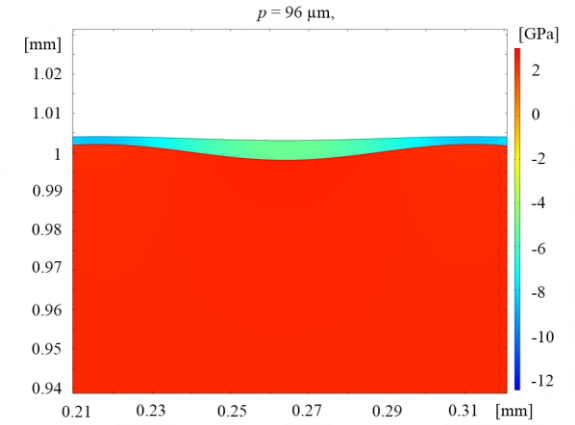

Figure 7: Illustration of the principle stress distribution for p = 96 µm

In Figure 7 the absolute maximum principle stress can be derived in the diamond layer above the upper vertexes of the steel surface. The maximum principle stress in the diamond coating is $\sigma_3 = -8.59$ GPa. The maximum shear stress at the line between the steel and the diamond is $\tau = 0.28$ GPa and the normal stress is calculated to be $\sigma_n = 0.07$ GPa.

Conclusion

By the help of the evaluated results it could be found, that with a larger period of the $f_1(x)$ and $f_2(x)$ functions, the absolute principle maximum stresses in the diamond layer reduces. With larger period of the $f_1(x)$ and $f_2(x)$ functions, the tensile stress disappears. Further simulations will be done to vary parameters like a_1 and a_2 as well as the thickness of the diamond layer, respectively. In future investigations, simulations will serve to derive trends for optimized surface microstructures of the substrate with the aim to reduce the residual stresses and thus preventing delamination. The results of the simulations will be compared with experimental results, so future simulation models can be improved and thus became even more complex.
Also, the consideration of the microstructure of the Y-Z plane will be of interest in future simulations. Conjectures suggest that at this Y-Z plane the residual stresses will be very interesting.

Acknowledgement

The project is funded by the German Research Foundation

DFG Deutsche Forschungsgemeinschaft
German Research Foundation

References

[1] J. J. Moore and D. Zhong, ‘Advanced Coatings for Structural Materials’, in *Encyclopedia of Materials: Science and Technology*, Elsevier, 2003, pp. 1–12

[2] L. Settineri, F. Bucciotti, F. Cesano, and M. G. Faga, ‘Surface Properties of Diamond Coatings for Cutting Tools’, *CIRP Ann.*, vol. 56, no. 1, pp. 573–576, 2007, ISSN: 00078506, DOI:10.1016/j.cirp.2007.05.137

[3] U. Wiklund, J. Gunnars, and S. Hogmark, ‘Influence of residual stresses on fracture and delamination of thin hard coatings’, *Wear*, vol. 232, no. 2, pp. 262–269, Oct. 1999, ISSN: 00431648, DOI:10.1016/S0043-1648(99)00155-6

[4] C. V. Thompson and R. Carel, ‘Stress and grain growth in thin films’, *J. Mech. Phys. Solids*, vol. 44, no. 5, pp. 657–673, May 1996, ISSN: 00225096, DOI:10.1016/0022-5096(96)00022-1

[5] R. Börner, S. Winkler, T. Junge, C. Titsch, A. Schubert, and W.-G. Drossel, ‘Generation of functional surfaces by using a simulation tool for surface prediction and micro structuring of cold-working steel with ultrasonic vibration assisted face milling’, *J. Mater. Process. Technol.*, vol. 255, no. August 2017, pp. 749–759, May 2018, ISSN: 09240136, DOI:10.1016/j.jmatprotec.2018.01.027

[6] A. Böge, *Handbuch Maschinenbau*. Wiesbaden: Springer Fachmedien Wiesbaden, 2013, ISBN: 978-3-658-06597-3, DOI: 10.1007/978-3-658-06598-0